



Open Archive TOULOUSE Archive Ouverte (OATAO)

OATAO is an open access repository that collects the work of Toulouse researchers and makes it freely available over the web where possible.

This is a publisher-deposited version published in: <http://oatao.univ-toulouse.fr/>
Eprints ID: 16124

To cite this version: Cardoso-Ribeiro, Flavio Luiz and Matignon, Denis and Pommier-Budinger, Valérie *Modeling by interconnection and control by damping injection of a fluid-structure system with non-collocated actuators and sensors*. (2016) In: International Conference on Noise and Vibration Engineering - ISMA 2016, 19 September 2016 - 21 September 2016 (Leuven, Belgium).

Any correspondence concerning this service should be sent to the repository administrator: staff-oatao@listes-diff.inp-toulouse.fr

Modeling by interconnection and control by damping injection of a fluid-structure system with non-collocated actuators and sensors

F.L. Cardoso-Ribeiro¹, D. Matignon¹, V. Pommier-Budinger¹

¹ Institut Supérieur de l'Aéronautique et de l'Espace (ISAE-SUPAERO),

Université de Toulouse, 31055 Toulouse Cedex 4, France

e-mail: flaviocr@ita.br

Abstract

This work addresses the modeling and control of fluid-structure systems. In the first part, the port-Hamiltonian systems (PHS) formulation is used for modeling fluid-structure interactions. This formulation allows describing fluid dynamics and structural dynamics separately and coupling the subsystems easily through physically relevant interconnection ports, which naturally arise in the PHS models. The modeling method is validated on the experimental set-up available at ISAE. The second part is devoted to the control of sloshing using damping injection, that is a classical passivity-based control method, in order to reduce vibrations in flexible structures. One difficulty of this approach is that collocated (and power conjugated) actuators and sensors are needed. This paper presents a method for dealing with damping injection in mechanical systems with non-collocated inputs/outputs making use of a state observer. Finally, control by damping injection is performed, and the overall method is successfully tested on the experimental device.

1 Introduction

The goal of optimizing the aircraft performance (reducing structural weight and increasing aerodynamic efficiency) is leading to airframes with increased structural flexibility. These new airplanes have vibration modes in the low-frequency range, which can couple with the rigid body motion, as well with the fuel sloshing inside the tanks. This coupling can potentially lead to reduced maneuverability, material fatigue or even instability and structural loss (see e.g. [1, Chapter 14] and [2]).

This paper is part of ongoing research on fluid-structure modeling and active control. A set up is available at ISAE, which consists of an aluminum plate with a water tank near the free tip. This device mimics the dynamics of a flexible wing with a fuel tank near the tip. The fluid and structural dynamics have similar natural vibration frequencies, leading to strong dynamic coupling between them. This structure can be controlled thanks to piezoelectric patches bonded on the clamped end of the plate.

In this paper, the port-Hamiltonian systems (PHS) formulation [3] is used for modeling and control the fluid-structure interactions of this device. A typical mathematical representation of port-Hamiltonian systems is given by:

$$\begin{cases} \dot{\mathbf{x}} &= J(\mathbf{x})\mathbf{e} + B\mathbf{u}, \\ \mathbf{y} &= B^T\mathbf{e} + D\mathbf{u}, \end{cases} \quad (1)$$

where $\mathbf{x}(t)$ is the vector of energy variables, $\mathbf{e} := \nabla_{\mathbf{x}}H(\mathbf{x})$ is the vector of co-energy variables, provided by the gradient of the system Hamiltonian ($H(\mathbf{x})$), \mathbf{u} is the input vector and \mathbf{y} is the output vector. $J(\mathbf{x})$ is the interconnection matrix and D is the feedthrough matrix; since both of them must be skew-symmetric, it is

easy to verify that:

$$\dot{H}(\mathbf{x}) = \mathbf{y}^T \mathbf{u}. \quad (2)$$

Many physical systems can be represented using this framework. In this paper, the interest of using PHS is twofold. Firstly, it provides a systematic way for modeling complex systems by the interconnection of simpler ones. Secondly, it provides a natural framework for passivity-based control techniques. Indeed, notice that a negative output-feedback such as $\mathbf{u} = -k\mathbf{y}$ ($k > 0$) gives:

$$\dot{H}(\mathbf{x}) = -k\mathbf{y}^T \mathbf{y} \leq 0 \quad \forall \mathbf{y}. \quad (3)$$

Provided that $H(\mathbf{x})$ is lower-bounded, this simple control law (called damping-injection) stabilizes the system. Mechanical systems can be controlled using this technique if the inputs and outputs are power-conjugated (the power flow is given by their product, as Eq. 2), which implies that they are collocated, i.e. the actuators and the sensors are located at the same place. Note that, conversely, collocated actuators and sensors do not necessarily give rise to power conjugated inputs and outputs. Due to the robustness properties, implementing control laws using collocated actuators and sensors is classical in the control of flexible structures (Ref. [4]). However, there are limitations to this approach when the inputs/outputs are not collocated and consequently not power-conjugated. For instance, in our fluid-structure application, the actuators are piezoelectric patches near the clamped end, and the sensors are accelerometers near the free end of the structure.

The use of passivity-based control techniques for non-passive linear systems was studied by Kelkar et. al in Refs. [5], [6] and [7]. They proposed “passivation” techniques by including series, feedback and feedforward compensators. Ref. [8] suggested an LMI-based method to find compensators that allow using PBC to non-passive systems. The design of state observers for a class of non-linear PHS has been addressed in Ref. [9].

This paper is organized as follows:

The interest of using the PHS formalism as a tool for modeling complex system by the interconnection of simpler ones is briefly recalled in Section 2. In Section 3, an observer-based controller is presented for non-conjugated mechanical systems. Firstly, the use of the PHS formalism allows identifying the conjugated inputs/outputs in a straightforward way. Secondly, a state observer is implemented to estimate the actuators conjugated output. Finally, Section 4 applied the techniques previously presented for modeling and control of the fluid-structure system.

2 Modeling by interconnection: an introduction to the port-Hamiltonian approach

2.1 Simple example: mass-spring coupling

As a very simple example of a mechanical system written using the port-Hamiltonian framework, let us consider a lumped mass with two forces F_1 and F_2 . The system Hamiltonian (total energy) is given by its kinetic energy:

$$H^m(p) = \frac{1}{2m} p^2, \quad (4)$$

where $p = mv$ is the particle momentum, m is the mass and v is the speed. The dynamic equations, obtained from Hamiltonian formulation, are given by:

$$\dot{p} = 0 \frac{\partial H^m}{\partial p} + \begin{bmatrix} 1 & 1 \end{bmatrix} \begin{bmatrix} F_1 \\ F_2 \end{bmatrix}, \quad (5)$$

$$\begin{bmatrix} v_1 \\ v_2 \end{bmatrix} = \begin{bmatrix} 1 \\ 1 \end{bmatrix} \frac{\partial H^m}{\partial p}. \quad (6)$$

Note that this system is written exactly as Eq. 1, where the inputs are the forces $\mathbf{u} = [F_1 \ F_2]^T$, the outputs are the speeds $[v_1 \ v_2]^T$, $J = 0$, $B = [1 \ 1]$. The energy variable is the momentum p , and the co-energy variable is the speed $\frac{\partial H^m}{\partial p} = v$. Besides, the Hamiltonian time-derivative is given by:

$$\dot{H}^m(p) = v_1 F_1 + v_2 F_2 = v(F_1 + F_2). \quad (7)$$

Similarly, consider a linear spring with displacement x , speed v_s and subject to a force F_s . The system Hamiltonian is provided by the potential energy:

$$H^s(x) = \frac{k}{2} x^2, \quad (8)$$

and the equations in the port-Hamiltonian framework are simply given by:

$$\dot{x} = 0 \frac{\partial H^s}{\partial x} + 1 v_s, \quad (9)$$

$$F_s = 1 \frac{\partial H^s}{\partial p}, \quad (10)$$

where now the input is the speed v_s , and the output is the spring force F_s . The energy variable is the spring displacement x , and the co-energy variable is the spring force $\frac{\partial H^s}{\partial x} = kx$. The time-derivative of the Hamiltonian is thus:

$$\dot{H}^s(x) = v_s F_s. \quad (11)$$

The mass and spring can be interconnected, by using the following kinematic and dynamic constraints:

$$\begin{aligned} v_s &= v_1, \\ F_s &= -F_1, \end{aligned} \quad (12)$$

which leads to the coupled equations:

$$\begin{aligned} \frac{d}{dt} \begin{bmatrix} p \\ x \end{bmatrix} &= \begin{bmatrix} 0 & -1 \\ 1 & 0 \end{bmatrix} \begin{bmatrix} \frac{\partial H}{\partial p} \\ \frac{\partial H}{\partial x} \end{bmatrix} + \begin{bmatrix} 1 \\ 0 \end{bmatrix} F_2, \\ \dot{x} &= [1 \ 0] \begin{bmatrix} \frac{\partial H}{\partial p} \\ \frac{\partial H}{\partial x} \end{bmatrix}. \end{aligned} \quad (13)$$

where $H(p, x) = H^m(p) + H^s(x)$. Notice that Eq. 13 is also a port-Hamiltonian system (as Eq. 1), with input port the force F_2 and output port the speed v_2 . One can easily verify that the energy exchange of this system is given by $\dot{H} = F_2 v_2$.

This simple example shows one of the interests of using the port-Hamiltonian formulation as a modeling tool. By interconnecting simple modules, the approach provides a systematic way for modeling more complex systems and guaranteeing the energy is preserved in each interconnection. In the previous example, only linear systems were considered. However, the same formalism can be used for nonlinear systems. For instance, a non-quadratic Hamiltonian could be used to represent the potential energy of the spring.

2.2 Interconnection of generic PHS

Let us now repeat the interconnection procedure for a more general example. Consider two PHSs written as:

$$\begin{aligned} \dot{\mathbf{x}}_1 &= (J_1 - R_1)\mathbf{e}_1 + B_{1,int}\mathbf{u}_{1,int} + B_{1,ext}\mathbf{u}_{2,ext}, & \dot{\mathbf{x}}_2 &= (J_2 - R_2)\mathbf{e}_2 + B_{2,int}\mathbf{u}_{2,int} + B_{2,ext}\mathbf{u}_{2,ext}, \\ \mathbf{y}_{1,int} &= B_{1,int}^T \mathbf{e}_1, & \mathbf{y}_{2,int} &= B_{2,int}^T \mathbf{e}_2, \\ \mathbf{y}_{1,ext} &= B_{1,ext}^T \mathbf{e}_1, & \mathbf{y}_{2,ext} &= B_{2,ext}^T \mathbf{e}_2, \end{aligned} \quad (14)$$

where $\mathbf{x}_i(t)$ ($i = 1, 2$) are the vectors of energy variables, $\mathbf{e}_i := \nabla_x H_i(\mathbf{x}_i)$ are the vectors of co-energy variables, given by the gradient of the system Hamiltonians ($H_i(\mathbf{x}_i)$). Each system has two pairs of input/output vectors, one that will be used for interconnection ($\mathbf{u}_{i,int}, \mathbf{y}_{i,int}$) and the other will be left for external interactions ($\mathbf{u}_{i,ext}, \mathbf{y}_{i,ext}$). As before, J_i are skewsymmetric matrices and R_i are positive semi-definite matrices.

There are two main power-preserving interconnections of interest during the coupling of physical systems. They are called "gyrator" and "transformer" interconnection. The "gyrator" interconnection is given by:

$$\begin{aligned}\mathbf{u}_{1,int} &= -C\mathbf{y}_{2,int}, \\ \mathbf{u}_{2,int} &= C^T\mathbf{y}_{1,int}.\end{aligned}\tag{15}$$

Since $\mathbf{u}_{1,int}^T\mathbf{y}_{1,int} + \mathbf{u}_{2,int}^T\mathbf{y}_{2,int} = 0$, this interconnection is power-preserving.

It is easy to verify that from this interconnection, we have:

$$\begin{aligned}\begin{bmatrix} \dot{\mathbf{x}}_1 \\ \dot{\mathbf{x}}_2 \end{bmatrix} &= \begin{bmatrix} J_1 - R_1 & -B_{1,int}C B_{2,int}^T \\ B_{2,int}C^T B_{1,int}^T & J_2 - R_2 \end{bmatrix} \begin{bmatrix} \mathbf{e}_1 \\ \mathbf{e}_2 \end{bmatrix} + \begin{bmatrix} B_{1,ext} & 0 \\ 0 & B_{2,ext} \end{bmatrix} \begin{bmatrix} \mathbf{u}_{1,ext} \\ \mathbf{u}_{2,ext} \end{bmatrix}, \\ \begin{bmatrix} \mathbf{y}_{1,ext} \\ \mathbf{y}_{2,ext} \end{bmatrix} &= \begin{bmatrix} B_{1,ext}^T & 0 \\ 0 & B_{2,ext}^T \end{bmatrix} \begin{bmatrix} \mathbf{e}_1 \\ \mathbf{e}_2 \end{bmatrix}\end{aligned}\tag{16}$$

where $H = H_1 + H_2$. Note that the ports used for interconnection totally disappear in the previous equation: the resulting PHS is explicit. The energy flow becomes dependent on the "external" ports only:

$$\dot{H} = \mathbf{u}_{1,ext}^T\mathbf{y}_{1,ext} + \mathbf{u}_{2,ext}^T\mathbf{y}_{2,ext}.\tag{17}$$

The "transformer" interconnection is given by:

$$\begin{aligned}\mathbf{u}_{1,int} &= -C\mathbf{u}_{2,int}, \\ \mathbf{y}_{2,int} &= C^T\mathbf{y}_{1,int}.\end{aligned}\tag{18}$$

Since $\mathbf{u}_{1,int}^T\mathbf{y}_{1,int} + \mathbf{u}_{2,int}^T\mathbf{y}_{2,int} = 0$, this interconnection is power-preserving.

In this case, the coupled system becomes:

$$\begin{aligned}\begin{bmatrix} \dot{\mathbf{x}}_1 \\ \dot{\mathbf{x}}_2 \end{bmatrix} &= \begin{bmatrix} J_1 - R_1 & 0 \\ 0 & J_2 - R_2 \end{bmatrix} \begin{bmatrix} \mathbf{e}_1 \\ \mathbf{e}_2 \end{bmatrix} + \begin{bmatrix} B_{1,ext} & 0 \\ 0 & B_{2,ext} \end{bmatrix} \begin{bmatrix} \mathbf{u}_{1,ext} \\ \mathbf{u}_{2,ext} \end{bmatrix} + \begin{bmatrix} -B_{1,int}C \\ B_{2,int} \end{bmatrix} \boldsymbol{\lambda}, \\ \begin{bmatrix} \mathbf{y}_{1,ext} \\ \mathbf{y}_{2,ext} \end{bmatrix} &= \begin{bmatrix} B_{1,ext}^T & 0 \\ 0 & B_{2,ext}^T \end{bmatrix} \begin{bmatrix} \mathbf{e}_1 \\ \mathbf{e}_2 \end{bmatrix}, \\ 0 &= \begin{bmatrix} -C^T B_{1,int}^T & B_{2,int}^T \end{bmatrix} \begin{bmatrix} \mathbf{e}_1 \\ \mathbf{e}_2 \end{bmatrix}.\end{aligned}\tag{19}$$

Eq. 19 is a Differential-Algebraic Equation (DAE), where $\boldsymbol{\lambda} = \mathbf{u}_{2,int}$ is the vector of Lagrange multipliers (unknowns) of the system. This system can be simulated using DAE solvers [10]. Other manipulations are also possible to avoid the constraints and find an equivalent set of ODE for this system. In the linear case, a reduced-order set of ODE can be obtained preserving the port-Hamiltonian structure of the system. These techniques are described in Ref. [11].

In the application presented in this paper (FSI), the system is described by partial differential equations (PDEs). Fortunately, an extension of the port-Hamiltonian framework to infinite-dimensional systems is available (see e.g. [12]). A simple example is presented in the next subsection.

2.3 Infinite-dimensional port-Hamiltonian systems

Let us consider the string equation:

$$\mu \frac{\partial^2 w}{\partial t^2} = \frac{\partial}{\partial z} \left(T \frac{\partial w}{\partial z} \right), \quad (20)$$

where μ is the string mass per unit length, $w(z, t)$ is the string deflection, T is the tension. After defining the following physically meaningful variables: $\alpha_1 := \mu \frac{\partial w}{\partial t}$, the linear moment density and $\alpha_2 := \frac{\partial w}{\partial z}$, the local string tangent angle, the system Hamiltonian (total energy) is computed:

$$H[\alpha_1, \alpha_2] = \frac{1}{2} \int_{z=0}^L \left(\frac{1}{\mu} \alpha_1^2 + T \alpha_2^2 \right) dz, \quad (21)$$

and the PDE can be rewritten as:

$$\frac{\partial}{\partial t} \begin{bmatrix} \alpha_1 \\ \alpha_2 \end{bmatrix} = \begin{bmatrix} 0 & \partial_z \\ \partial_z & 0 \end{bmatrix} \begin{bmatrix} e_1 \\ e_2 \end{bmatrix}, \quad (22)$$

where $e_i(z, t) := \frac{\delta H}{\delta \alpha_i}$ is the variational derivative¹ of H with respect to α_i . It is straightforward to verify that the energy flow of this system depends only on the boundary conditions:

$$\dot{H} = e_1(L, t)e_2(L, t) - e_1(0, t)e_2(0, t). \quad (23)$$

This motivated the definition of physically meaningful *boundary ports*, in this case given by $e_1 = \frac{\delta H}{\delta \alpha_1} = \frac{\alpha_1}{\mu} = \frac{\partial w}{\partial t}$ (the vertical speed), and $e_2 = \frac{\delta H}{\delta \alpha_2} = T \alpha_2 = T \frac{\partial w}{\partial z}$ (the vertical component of force), both evaluated at the boundary. One possible choice of input/output ports² is the following: $\mathbf{u}_\partial = [e_1(L, t), -e_2(0, t)]^T$ and $\mathbf{y}_\partial = [e_2(L, t), e_1(0, t)]^T$. Then, just like in the finite-dimensional case, Eq. 23 rewrites as $\dot{H} = \mathbf{y}_\partial^T \mathbf{u}_\partial$.

Finally, there are several methods for semi-discretization in space that allow obtaining a finite-dimensional approximation of infinite-dimensional port-Hamiltonian systems that preserves the port-Hamiltonian structure of the system (and the semi-discretized equations can be rewritten as Eq. 1). For these methods, see e.g. Refs. [14, 15].

In Section 4 of this paper, we present the infinite-dimensional port-Hamiltonian equations of each element of the system. Then, each system is independently semi-discretized leading to “modules” represented by finite-dimensional PHS (as Eq. 1). Finally, the “gyrator” and “transformer” interconnections are used to couple all the modules of the system. The final system can thus be used for simulation and control design.

3 Control by damping injection for non-collocated actuators and sensors

3.1 Defining a port-Hamiltonian system

This study will be limited to linear systems. For these systems, the Hamiltonian is given by the quadratic form: $H(\mathbf{x}) = \frac{1}{2} \mathbf{x}^T Q \mathbf{x}$, where $\mathbf{x} \in \mathbb{R}^n$ is the energy variables vector and Q is an $n \times n$ symmetric positive-definite matrix. The Hamiltonian gradient is given by $\nabla_{\mathbf{x}} H(\mathbf{x}) = Q \mathbf{x}$. We assume that the system dynamics is given by:

$$\begin{aligned} \dot{\mathbf{x}} &= (J - R)Q\mathbf{x} + B_a \mathbf{u}_a, \\ \mathbf{y}_s &= B_s^T Q \mathbf{x}, \end{aligned} \quad (24)$$

¹See e.g. Chapter 4 of Ref. [13] for the definition of variational derivative.

²Other choices are possible, see e.g. Ref. [12].

where J is an $n \times n$ skew-symmetric matrix and R is an $n \times n$ positive semi-definite matrix; $\mathbf{u}_a \in \mathbb{R}^{n_a}$ is the actuators input vector, hence subscript “a” stands for actuators; $\mathbf{y}_s \in \mathbb{R}^{n_s}$ is the sensors output vector, similarly subscript “s” stands for sensors; B_a and B_s are $n \times n_a$ and $n \times n_s$ matrices, respectively. Note that the previous system is not strictly speaking port-Hamiltonian, since $B_a \neq B_s$. Note also that the input \mathbf{u}_a and output \mathbf{y}_s are not conjugated. If we compute the Hamiltonian time-derivative, we find:

$$\dot{H} = (\mathbf{x}^T Q B_a) \mathbf{u}_a - \mathbf{x}^T Q R Q \mathbf{x} \leq (\mathbf{x}^T Q B_a) \mathbf{u}_a \neq \mathbf{y}_s^T \mathbf{u}_a. \quad (25)$$

This motivates us to define $\mathbf{y}_a := B_a^T Q \mathbf{x} \in \mathbb{R}^{n_a}$, which is the conjugated output of \mathbf{u}_a . Since this variable cannot actually be measured, we call it a *virtual* output. In order to write the equations using the classical port-Hamiltonian formalism, we also introduce another *virtual* variable, $\mathbf{u}_s \in \mathbb{R}^{n_s}$ which is the conjugated input of the sensors (actually $\mathbf{u}_s = 0$). With these extra *virtual* ports at hand, the original system (Eq. 24) now takes the more classical pHs form below:

$$\begin{aligned} \dot{\mathbf{x}} &= (J - R)Q\mathbf{x} + \begin{bmatrix} B_a & B_s \end{bmatrix} \begin{bmatrix} \mathbf{u}_a \\ \mathbf{u}_s \end{bmatrix}, \\ \begin{bmatrix} \mathbf{y}_a \\ \mathbf{y}_s \end{bmatrix} &= \begin{bmatrix} B_a^T \\ B_s^T \end{bmatrix} Q\mathbf{x}, \end{aligned} \quad (26)$$

which is written as Eq. 1. The time derivative of the Hamiltonian is then:

$$\dot{H} = \mathbf{y}_a^T \mathbf{u}_a + \mathbf{y}_s^T \mathbf{u}_s - \mathbf{x}^T Q R Q \mathbf{x}. \quad (27)$$

Since $\mathbf{u}_s = 0$:

$$\dot{H} = \mathbf{y}_a^T \mathbf{u}_a - \mathbf{x}^T Q R Q \mathbf{x}. \quad (28)$$

3.2 Designing an observer

In Eq. 26, \mathbf{y}_a is not being measured. For using passivity-based control, it is necessary to estimate it. For this purpose, a state observer of the system is computed.

Hypothesis 1. *The pair $((J - R)Q, B_s^T Q)$ is assumed to be observable.*

The classical Luenberger continuous state observer is given by:

$$\begin{aligned} \dot{\hat{\mathbf{x}}} &= (J - R)Q\hat{\mathbf{x}} + B_a \mathbf{u}_a + L(\mathbf{y}_s - B_s^T Q\hat{\mathbf{x}}), \\ \hat{\mathbf{y}}_a &= B_a^T Q\hat{\mathbf{x}}, \quad \hat{\mathbf{x}}(0) = 0. \end{aligned} \quad (29)$$

The observer error ($\mathbf{e} = \mathbf{x} - \hat{\mathbf{x}}$) dynamics is given by:

$$\dot{\mathbf{e}} = (J - R - L B_s^T) Q \mathbf{e}. \quad (30)$$

The matrix L should be designed such that the error dynamics be asymptotically stable (e.g. using pole placement). The fact that Eq. 30 is independent of the control input leads to the well-known principle of separation of estimation and control (Ref. [16]).

3.3 Designing a control law

The damping injection control law is given by $\mathbf{u}_a = -K_a \mathbf{y}_a = -K_a B_a^T Q \mathbf{x}$, where K_a is an $n_a \times n_a$ matrix. Using this law with the *theoretical* system (Eq. 26), the closed-loop dynamics becomes:

$$\dot{\mathbf{x}} = (J - R - B_a K_a B_a^T) Q \mathbf{x}. \quad (31)$$

Property 1. *The closed-loop system is stable for any symmetric positive-definite matrix K_a .*

Proof. The Hamiltonian rate of change of Eq. 28, with $\mathbf{u}_a = -K_a \mathbf{y}_a$ and $\mathbf{y}_a = B_a^T Q \mathbf{x}$ is given by:

$$\dot{H}(\mathbf{x}) = -\mathbf{y}_a^T K_a \mathbf{y}_a - \mathbf{x}^T Q R Q \mathbf{x}, \quad (32)$$

$$= -(Q\mathbf{x})^T (B_a K_a B_a^T + R) (Q\mathbf{x}) \leq 0. \quad (33)$$

Using this control law, we can guarantee that the system energy will never increase. Since the Hamiltonian has a lower bound, it guarantees that the system is stable. In addition, Eq. 33 shows that $B_a K_a B_a^T + R \geq 0$ is a sufficient condition for stability. \square

3.4 Observer-based controller

Since \mathbf{y}_a is not being measured, we will use its estimate $\hat{\mathbf{y}}_a$ to define the new control law:

$$\mathbf{u}_a := -K_a \hat{\mathbf{y}}_a = -K_a B_a^T Q \hat{\mathbf{x}}, \quad (34)$$

with positive-definite matrix K_a .

Property 2. *The dynamical system (Eq. 24) together with the state observer (Eq. 29) and the controller (Eq. 34) is stable for any positive-definite K_a .*

Proof. This can be easily verified from the separation principle. For the sake of completeness, we recall the proof here. The closed-loop equations are given by:

$$\begin{bmatrix} \dot{\mathbf{e}} \\ \dot{\mathbf{x}} \end{bmatrix} = \begin{bmatrix} (J - R - L B_s^T)Q & 0 \\ -B_a K_a B_a^T Q & (J - R - B_a K_a B_a^T)Q \end{bmatrix} \begin{bmatrix} \mathbf{e} \\ \mathbf{x} \end{bmatrix} \quad (35)$$

Note that since the state matrix is block-triangular, the eigenvalues of the full system are given by the eigenvalues of the observer $(J - R - L B_s^T)Q$ and of the closed-loop plant without the observer $(J - R - B_a K_a B_a^T)Q$. For this reason, provided that the observer is stable by design, and the closed-loop plant without observer is stable (Property 1), the closed-loop system with observer is also stable. \square

Remark 1. *The proposed controller can be seen as a particular case of state feedback, with a reduced number of degrees of freedom. Note that usual state feedback is given by $\mathbf{u}_a = -K \hat{\mathbf{x}}$, where K is an $n_a \times n$ matrix. Our controller implies the following structure for the gain $K = K_a B_a^T Q$. The structure of the state feedback gain is physically motivated to remove energy from the system (increase damping). Since K_a is an $n_a \times n_a$ positive-definite matrix, a diagonal matrix with positive elements stabilizes the system, making the control design simpler, from a control practitioner perspective.*

4 Application to a fluid-structure system

An active flexible structure that consists of a free-clamped plate with a tip tank partially filled with fluid controlled by two piezoelectric patches attached near the fixed end is used to validate the modeling and control strategy (Figs. 1). The movement of the plate is measured using an accelerometer located near the plate free-tip.

In this section, firstly the modeling of the system is described in §4.1, then the control methodology presented in the previous section is applied for this system in §4.2.

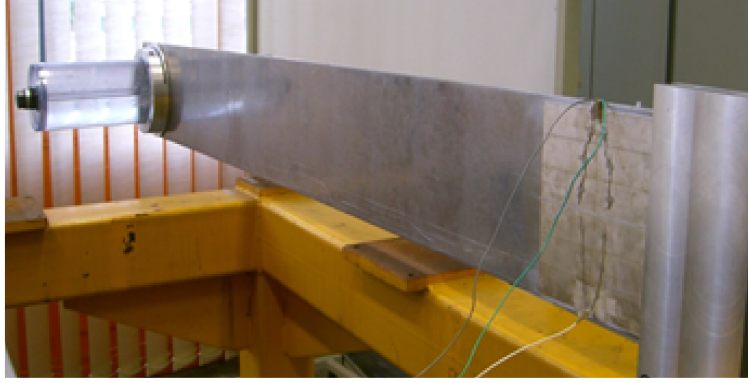


Figure 1: Photo of the flexible plate with tip tank partially filled with water. The piezoelectric patches are attached to the structure near the clamped end.

4.1 Modeling

The modeling of the experimental device is done using the port-Hamiltonian approach. The beam is represented by the Euler-Bernoulli equation in §4.1.1. The tank is assumed to be a rigid body (§4.1.2). Finally, the fluid is represented by Saint-Venant equations (§4.1.3). The coupling, using the interconnection ports previously defined, is thus presented in §4.1.4. Finally, numerical results and experimental validation are presented in §4.1.5.

4.1.1 Bending equations

The simplest mathematical representation of beam vibration in bending is given by the Euler-Bernoulli equation:

$$\mu(z)\ddot{w} = -\partial_{z^2}^2 (EI(z)\partial_{z^2}^2 w) + \partial_{z^2}^2 (\Pi_{ab}(z)k_p v(t)) , \quad (36)$$

where $w(z, t)$ is the beam deflection at point z ($0 \leq z \leq L$) and time t , $\mu(z)$ the beam mass per unit length, E the material Young Modulus, I the section inertia, v the voltage applied to the piezoelectric patch, k_p an electromechanical coupling constant, L the beam length. $\Pi_{ab}(z)$ is a rectangular function, that is equal to 1 inside the piezoelectric patch ($a \leq z \leq b$) and 0 elsewhere.

The system Hamiltonian is given by:

$$H^B[x_1^B, x_2^B] = \frac{1}{2} \int_{z=0}^L \left(\frac{x_1^B(z, t)^2}{\mu(z)} + EI(z)x_2^B(z, t)^2 \right) dz , \quad (37)$$

where $x_1(z, t)$ and $x_2(z, t)$ are the energy variables, defined as $x_1^B(z, t) := \mu(z)\dot{w}(z, t)$ and $x_2^B(z, t) := \partial_{z^2}^2 w(z, t)$.

The variational derivatives of the Hamiltonian with respect to x_1^B and x_2^B are given by:

$$\begin{aligned} e_1^B(z, t) &:= \frac{\delta H^B}{\delta x_1} = \frac{x_1^B(z, t)}{\mu} = \dot{w}(z, t) \\ e_2^B(z, t) &:= \frac{\delta H^B}{\delta x_2} = EI(z)x_2^B(z, t) = EI\partial_{z^2}^2 w . \end{aligned} \quad (38)$$

Note that e_1^B is the local vertical speed, and e_2^B is the local bending moment. Eq. 36 can thus be rewritten as:

$$\begin{bmatrix} \dot{x}_1^B \\ \dot{x}_2^B \end{bmatrix} = \begin{bmatrix} 0 & -\partial_{z^2}^2 \\ \partial_{z^2}^2 & 0 \end{bmatrix} \begin{bmatrix} e_1^B \\ e_2^B \end{bmatrix} + \begin{bmatrix} \partial_{z^2}^2 \\ 0 \end{bmatrix} \Pi_{ab}(z)k_p v(t) , \quad (39)$$

The time-derivative of the Hamiltonian is given as:

$$\dot{H}^B = (\mathbf{y}^B)^T \mathbf{u}^B, \quad (40)$$

where one possible definition of the input/output vector is:

$$\mathbf{y}^B := \begin{bmatrix} \partial_z \mathbf{e}_2(0) \\ -\mathbf{e}_2(0) \\ -\mathbf{e}_1(L) \\ \partial_z \mathbf{e}_1(L) \\ v^* \end{bmatrix}, \quad \mathbf{u}^B = \begin{bmatrix} \mathbf{e}_1(0) \\ \partial_z \mathbf{e}_1(0) \\ \partial_z \mathbf{e}_2(L) \\ \mathbf{e}_2(L) \\ v \end{bmatrix}. \quad (41)$$

Note that the energy flow depends on the boundary values of e_1 (vertical speed), e_2 (moment), $\partial_z e_1$ (rotation speed) and $\partial_z e_2$ (force). In addition, it depends on the applied voltage and its conjugate value $v^* := k_p (\partial_z e_1(b) - \partial_z e_1(a))$ (which is the mechanically induced current).

4.1.2 Rigid body

A rigid tank with two degrees of freedom is considered, one related to translation $w_B(t)$ and the other related to rotation $\theta_B(t)$ due to bending. In this case, the Hamiltonian of the rigid body is equal to the kinetic energy:

$$H^{RB}(p, p_{\theta B}) = \frac{1}{2} \left(\frac{p^2}{m_{RB}} + \frac{p_{\theta B}^2}{I_{RB}^B} \right), \quad (42)$$

where p and $p_{\theta B}$ are the moment variables defined as $p := m_{RB} \dot{w}_B$ and $p_{\theta B} := I_{RB}^B \dot{\theta}_B$, m_{RB} the mass and I_{RB} the rotational inertia.

The rigid body equations can be written as port-Hamiltonian systems:

$$\dot{p} = 0 \partial_p H^{RB} + F_{\text{ext}}, \quad (43)$$

$$\dot{p}_{\theta B} = 0 \partial_{p_{\theta B}} H^{RB} + M_{\text{ext},B}, \quad (44)$$

where F_{ext} is the sum of forces applied to the tank and $M_{\text{ext},B}$ the sum of moments in bending direction, which are the inputs of the system. Their conjugated outputs are $\dot{w}_B = \partial_p H^{RB}$ and $\dot{\theta}_B = \partial_{p_{\theta B}} H^{RB}$. The rate of change of the Hamiltonian is given by:

$$\dot{H}^{RB} = (\mathbf{u}^{RB})^T \mathbf{y}^{RB}, \quad (45)$$

where $\mathbf{u}^{RB} = [F_{\text{ext}}, M_{\text{ext},B}]^T$ and $\mathbf{y}^{RB} = [\dot{w}_B, \dot{\theta}_B]^T$.

4.1.3 Sloshing

The following hypotheses will be assumed for the fluid equations: non-viscous, incompressible fluid and little depth of fluid in comparison to the tank length (for this reason, these equations are also known as *shallow water* equations). A derivation of Saint-Venant equations for tanks under rigid-body motion is presented in [17]. Here, a linearized version with translation only will be used.

Let us define the following variables to describe the fluid motion: $v(z, t)$ is the fluid speed at point z ($-a/2 \leq z \leq a/2$) and time t ; $\tilde{h}(z, t)$ is the fluid height relative to static equilibrium height \bar{h} (the total height is thus $h(z, t) = \bar{h} + \tilde{h}(z, t)$).

The Hamiltonian is given by:

$$H^F := \int_{-a/2}^{a/2} \left(\rho b g \bar{h}^2 \frac{\alpha_1^2}{2} + \frac{\alpha_2^2}{2 \rho \bar{h} b} \right) dz. \quad (46)$$

where $\alpha_1 := \frac{\bar{h}}{h}$ is the relative height and $\alpha_2 := \rho \bar{h} b v$ the mass flow rate.

The co-energy variables are given by the variational derivative of H^F with respect to the infinite-dimensional energy variables $\alpha_1(z, t)$ and $\alpha_2(z, t)$:

$$e_1^F(z, t) := \frac{\delta}{\delta \alpha_1} H^f = \rho b g \bar{h}^2 \alpha_1 = \rho b g \bar{h} \tilde{h}, \quad (47)$$

$$e_2^F(z, t) := \frac{\delta}{\delta \alpha_2} H^f = \frac{\alpha_2}{\rho \bar{h} b} = v. \quad (48)$$

Notice that $e_1^F(z, t)$ is the local pressure relative to equilibrium ($\rho g \bar{h}$) multiplied by the fluid section area ($b \bar{h}$) (so, it is equivalent to an “incremental” force due to pressure) and $e_2^F(z, t)$ is the local fluid speed.

The Saint-Venant equations using these variables are given by:

$$\frac{\partial}{\partial t} \begin{bmatrix} \alpha_1 \\ \alpha_2 \end{bmatrix} = \begin{bmatrix} 0 & -\partial_z \\ -\partial_z & 0 \end{bmatrix} \begin{bmatrix} e_1^F \\ e_2^F \end{bmatrix}. \quad (49)$$

The time-derivative of H^F can be computed as:

$$\dot{H}^F = (\mathbf{u}^F)^T \mathbf{y}^F, \quad (50)$$

where $\mathbf{u}^F = [-e_1(a/2, t), e_2^F(-a/2, t)]^T$ and $\mathbf{y}^F = [e_2^F(a/2, t), e_1^F(-a/2, t)]^T$. Again, notice that the rate of change of the Hamiltonian is a function of the interconnection ports, i.e. the boundary conditions (speed and force applied to the tank walls).

4.1.4 Coupling

It is now time to couple all the elements of the system. First, we notice that several kinematic constraints appear, due to the coupling at the interconnection point:

- Translation speeds of each subsystem are equal (3 constraints):

$$\dot{w}_B = e_2^B(L, t) = e_2^F(-a/2, t) = e_2^F(a/2, t). \quad (51)$$

- Rotation speeds in bending are equal (1 constraint):

$$\dot{\theta}_B = \frac{\partial e_2^B}{\partial z}(L, t). \quad (52)$$

The Hamiltonian of the global system is given by the sum of each Hamiltonian component (Eqs. 37, 42 and 46):

$$H = H^B + H^{RB} + H^F. \quad (53)$$

Then, by using the sum of each Hamiltonian component rate of change (Eqs. 40, 45 and 50), and imposing the previous kinematic constraints, the following global Hamiltonian rate of change is obtained:

$$\dot{H} = +\dot{w}_B \underbrace{\left(-\frac{\partial}{\partial z} e_1^B(L, t) + F_{\text{ext}} - e_1^F(a/2, t) + e_1^F(-a/2, t) \right)}_{F_\Sigma} + \dot{\theta}_B \underbrace{(e_1^B(L, t) + M_{\text{ext},B})}_{M_{\Sigma,B}} + v(t)v^*(t). \quad (54)$$

Notice that F_Σ and $M_{\Sigma,B}$ are the sum of external forces/moments applied to each subsystem. From a global system perspective, they are the sum of internal forces/moments at the interconnection point, which should be equal to zero:

$$F_\Sigma = 0, \quad M_{\Sigma,B} = 0. \quad (55)$$

With these kinematic and dynamic constraints, the rate of change of the Hamiltonian is given by $\dot{H} = v(t)^*v(t)$.

4.1.5 Obtaining the finite-dimensional PHS

The following steps are followed in order to obtain a finite-dimensional representation of the coupled system, as Eq. 26:

1. The beam (§4.1.1) and fluid equations (§4.1.3) are semi-discretized using the method presented in Refs. [15, 18]. Thus, each of the systems is represented as Eq. 1, keeping the same input and output ports defined for the infinite-dimensional systems;
2. The modules are coupled using the interconnections presented in §2.2, leading to a constrained port-Hamiltonian system (similar to Eq. 19);
3. Finally, the constraints are removed (as in Ref. [11]), leading to a numerical model written as an explicit port-Hamiltonian system in the form of Eq. 26. The actuator input port is given by the applied voltage $v(t)$ (and its “virtual” output $v^*(t)$). The sensor output is the speed at the tip of the beam (and its conjugated input is a “virtual” collocated force).

To validate the modeling approach presented in this paper, the natural frequencies and the frequency response obtained from experiments were compared to results from the numerical model. Fig. 2 presents the frequency response, and Table 1 presents the natural frequencies, both for the tank 25% filled. Note that a good agreement between the numerical and experimental results is obtained. Modes 1 to 5 are mainly related to coupling between the sloshing modes and the first bending mode. Mode 6 is related to torsion, which was not modeled in this work. Modes 7 and 8 are related to bending.

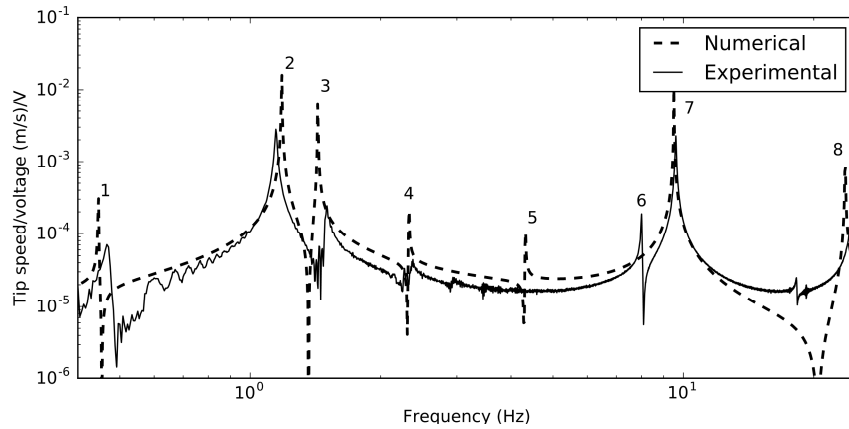


Figure 2: Frequency response: comparison between numerical and experimental results. The input is the voltage applied to the piezoelectric patches, the output is the tip speed evaluated from the measured acceleration. Tank 25% filled with water.

The resulting finite-dimensional model can thus be used for control design with the method described in Section 3. The results are presented in the next section.

Mode	Description	Frequency (Hz)	
		Numerical	Experimental
1	1st sloshing + 1st bending	0.43	0.47
2	2nd sloshing + 1st bending	1.18	1.15
3	3rd sloshing + 1st bending	1.43	1.50
4	4th sloshing + 1st bending	2.32	2.38
5	5th sloshing + 1st bending	4.32	2.94
6	1st torsion		8.01
7	2nd bending	9.51	9.61
8	3rd bending	23.63	24.63

Table 1: Comparison between the natural frequencies obtained experimentally and numerically.

4.2 Control by damping injection using an observer

The proposed observer based controller was tested on the experimental device. The controller was implemented using MATLAB Simulink, on Real-time Windows Target, with an NI 6024-E board. A sample time of 0.001 s was chosen. One 4371 Bruel & Kjaer accelerometer was used (located near the plate free tip), together with a charge amplifier (Type 2635). The amplifier can give directly the speed measurements but only for frequencies above 1 Hz. The two PZT piezoelectric actuators were actuated symmetrically.

Once the observer was designed, the plant behavior was tested for different values of the controller gain k_a . Frequency response from 1 to 26 Hz is shown in Fig. 3. A reduction of the peaks when using the controller shows that it introduces damping in the system. The damping ratios of three modes that are attenuated by the controllers are presented in Table 2.

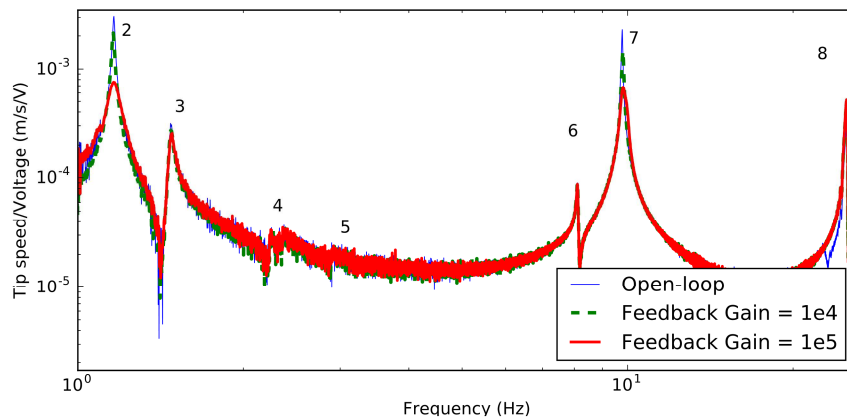


Figure 3: Experimental frequency response for different gains.

Mode	Description	Open-loop	Damping ratio	
			Open-loop	Closed-loop
			Gain = 10^4	Gain = 10^5
2	2nd sloshing + 1st bending	0.0045	0.0054	0.0150
3	3rd sloshing + 1st bending	0.0053	0.0058	0.0090
7	2nd bending	0.0020	0.0035	0.0095

Table 2: Comparison between damping ratios obtained experimentally.

Figures 4 and 5 show the time response of the system initially excited during 20 seconds with no control using a harmonic voltage, at two different frequencies (near the natural frequencies of modes 2 and 9, respectively),

and then controlled according to the proposed strategy. The time-response shows the decrease of the speed for different values of k_a .

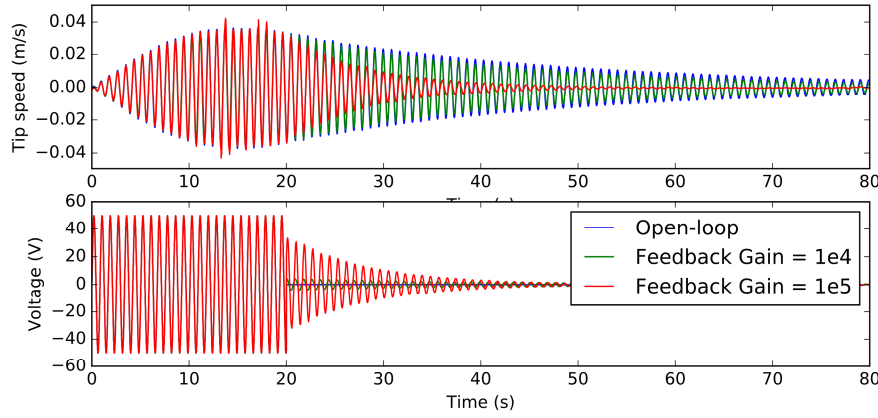


Figure 4: Experimental time response for different gains: the system is excited using a sinusoidal voltage at 1.2 Hz for the first 20 seconds; then, the control law is activated. Top: tip deflection speed; Bottom: Actuator voltage.

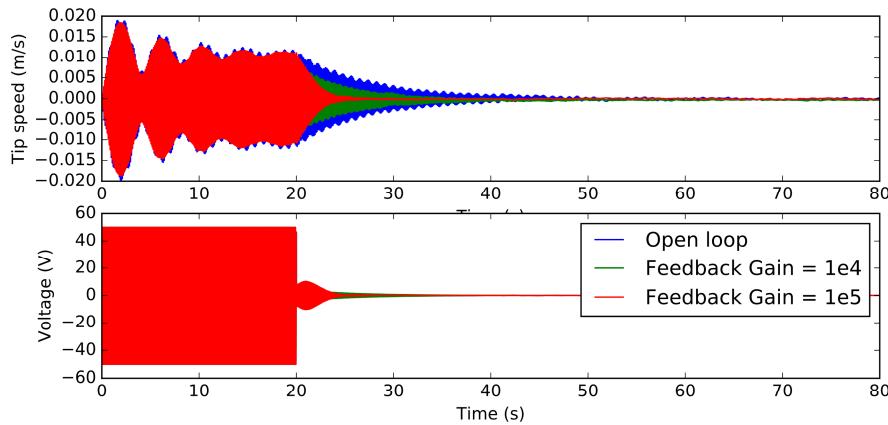


Figure 5: Experimental time response for different gains: the system is excited using a sinusoidal voltage at 9.5 Hz for the first 20 seconds; then, the control law is activated. Top: tip deflection speed; Bottom: Actuator voltage.

5 Conclusions and perspectives

This paper focuses on the use of the port-Hamiltonian systems for the modeling and control of a fluid-structure system. Firstly, we presented the interest of this technique from a modeling point of view: it provides a framework that allows interconnecting models in a straightforward and physically meaningful way. The method was used to model a fluid-structure system. Secondly, this paper shows a technique for damping-injection in mechanical systems with non-collocated inputs/outputs. The idea is to take advantage of the port-Hamiltonian formalism and to use a state observer that allows estimating the conjugated ports of the actuators. Then, classical damping injection techniques are used.

It is important to recall that the structure of the proposed controller is the same as the usual state feedback with state observer, presented in Fig. 6 (used for reducing vibrations in Refs. [19] and [20]). The difference

lies in the fact that the observer is written in such a way that the state vector is the vector of energy variables (Eq. 29). The control gain K is now strongly structured as $K = k_a B_a^T Q$, and the closed-loop system proves stable for any positive k_a . Note that this choice of gain is physically motivated to increase the structural damping. The method is an alternative way of finding the feedback gain K , with a reduced number of degrees of freedom.

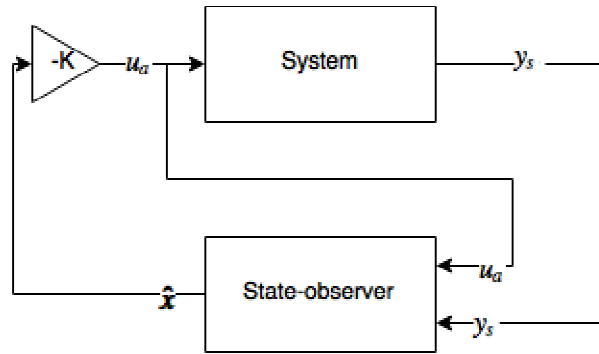


Figure 6: Observer-based control with state feedback.

The method was tested on an experimental device and promising results were obtained. Although only one input and one output were used in the experiment, the methodology proposed in Section 3 can also be used for MIMO systems.

One limitation of the proposed method is that a precise dynamical model of the plant is necessary to compute the observer dynamics. Further work should be done to analyze the robustness characteristics of this control technique. In particular, we should focus on how to design the state observer to improve the system robustness to modeling uncertainties.

Acknowledgments

This work was partially supported by ANR-project HAMECMOPSYs ANR-11-BS03-0002. The author F. L. Cardoso-Ribeiro is on leave from the Instituto Tecnológico de Aeronáutica with financial support from CNPq - Brazil.

References

- [1] M. J. Abzug, E. E. Larrabee. *Airplane Stability and Control, Second Edition*. Cambridge University Press, Cambridge (2002).
- [2] C. Farhat, E. K. Chiu, D. Amsallem, J.-S. Schotté, R. Ohayon. *Modeling of Fuel Sloshing and its Physical Effects on Flutter*. AIAA Journal (2013), Vol. 51, No. 9, pp. 2252–2265.
- [3] A. J. van der Schaft, D. Jeltsema. *Port-Hamiltonian Systems Theory: An Introductory Overview*. Foundations and Trends in Systems and Control (2014), Vol. 1, No. 2, pp. 173–378.
- [4] A. Preumont. *Vibration Control of Active Structures*, volume 179. Springer (2011).
- [5] A.G. Kelkar, S.N. Joshi. *Robust control of non-passive systems via passification*. In *Proceedings of the 1997 American Control Conference (ACC)*, Albuquerque, NM, United States (1997), pp. 2657–2661.

- [6] A.G. Kelkar, S.M. Joshi. *Robust passification and control of non-passive systems*. In *Proceedings of the 1998 American Control Conference (ACC)*, Philadelphia, PA, United States (1998), pp. 3133–3137.
- [7] A. G. Kelkar, S. M. Joshi. *Control of Elastic Systems via Passivity-Based Methods*. *Journal of Vibration and Control* (2004), Vol. 10, No. 11, pp. 1699–1735.
- [8] A.G. Kelkar, Y. Mao, S.M. Joshi. *LMI-based passification for control of non-passive systems*. In *Proceedings of the 2000 American Control Conference (ACC)*, Chicago, IL, United States (2000), pp. 1271–1275.
- [9] A. Venkatraman, A. J. van der Schaft. *Full-order observer design for a class of port-Hamiltonian systems*. *Automatica* (2010), Vol. 46, No. 3, pp. 555–561.
- [10] P. Kunkel, V. Mehrmann. *Differential-Algebraic Equations: Analysis and Numerical Solution*. European Mathematical Society (2006).
- [11] A. J. van der Schaft. *Port-Hamiltonian Differential-Algebraic Systems*. In *Surveys in Differential-Algebraic Equations I*, Springer (2013), pp. 173–226
- [12] Y. Le Gorrec, H. Zwart, B. Maschke. *Dirac structures and Boundary Control Systems associated with Skew-Symmetric Differential Operators*. *SIAM Journal on Control and Optimization* (2005), Vol. 44, No. 5, pp. 1864–1892.
- [13] V. Duindam, A. Macchelli, S. Stramigioli, H. Bruyninckx. *Modeling and Control of Complex Physical Systems: The Port-Hamiltonian Approach*. Springer Berlin Heidelberg, Berlin, Heidelberg (2009).
- [14] G. Golo, V. Talasila, A. J. van der Schaft, B. Maschke. *Hamiltonian discretization of boundary control systems*. *Automatica* (2004), Vol. 40, No. 5, pp. 757–771.
- [15] R. Moulla, L. Lefevre, B. Maschke. *Pseudo-spectral methods for the spatial symplectic reduction of open systems of conservation laws*. *Journal of Computational Physics* (2012), Vol. 231, No. 4, pp. 1272–1292.
- [16] D. Luenberger. *Observers for multivariable systems*. *IEEE Transactions on Automatic Control* (1966), Vol. 11, No. 2, pp. 190–197.
- [17] N. Petit, P. Rouchon. *Dynamics and solutions to some control problems for water-tank systems*. *IEEE Transactions on Automatic Control* (2002), Vol. 47, No. 4, pp. 594–609.
- [18] F. L. Cardoso-Ribeiro, D. Matignon, V. Pommier-Budinger. *Piezoelectric beam with distributed control ports : a power-preserving discretization using weak formulation*. In *2nd IFAC Workshop on Control of Systems Governed by Partial Differential Equations (Invited Session)*, Bertinoro, Italy (2016).
- [19] G. S. Aglietti, S. B. Gabriel, R. S. Langley, E. Rogers. *A modeling technique for active control design studies with application to spacecraft microvibrations*. *The Journal of the Acoustical Society of America* (1997), Vol. 102, No. 4, pp. 2158–66.
- [20] J. Zhang, L. He, E. Wang, R. Gao. *A LQR Controller Design for Active Vibration Control of Flexible Structures*. 2008 IEEE Pacific-Asia Workshop on Computational Intelligence and Industrial Application (2008), pp. 127–132.